Materials Chemistry and Physics 177 (2016) 505–511

Contents lists available at ScienceDirect

Materials Chemistry and Physics

journal homepage: www.elsevier.com/locate/matchemphys

Processing and thermoluminescent response of porous biomorphic dysprosium doped yttrium disilicate burner

S.C. Santos*, C. Yamagata, L.L. Campos, S.R.H. Mello-Castanho

Instituto de Pesquisas Energeticas e Nucleares – IPEN, Cidade Universitaria, Av. Prof. Lineu Prestes 2242, Sao Paulo, Brazil

HIGHLIGHTS

- Bio-prototyping of yttrium disilicate burner is reported.
- The effect of Dy^{3+} on thermoluminescent response of yttrium disilicate is discussed.
- Radiant efficiency of the biomorphic yttrium disilicate burner is evaluated.

ARTICLE INFO

Article history:
Received 12 February 2016
Received in revised form
6 April 2016
Accepted 18 April 2016
Available online 23 April 2016

Keywords:
Microporous materials
Nanostructures
Ceramics
Coatings
Luminescence

ABSTRACT

The present study reports a process to develop a porous biomorphic dysprosium doped yttrium disilicate burner from biotemplating of Luffa Cylindrica and its thermoluminescent response is evaluated. Processing parameters such as rheological behavior of the ceramic suspensions, surface chemistry of the nanoparticles, microstructure, thermal stability of the biotemplating, as well as thermoluminescent response of the nanoparticles, were investigated. Ceramic suspensions prepared at pH 10 from tetramethylammonium hydroxide, 2 wt% polyacrylic ammonium salt and 0.4 wt% carboxymethylcellulose exhibited shear thinning behavior, suitable apparent viscosity for replica method and porous microstructure as sintered. Promising thermoluminescent result of the yttrium disilicate nanoparticles was observed at 580 nm and at 180 °C. The burner prototype sintered at 1500 °C for 7 h exhibited reticulated shape similar to biotemplating, porous microstructure with mean grain size around 1 μm, no apparent cracks, pycnometric density of 3.21 g cm^{-3} (80% of theoretical density; 4.04 g cm^{-3}) and radiant efficiency of 13%. These results show that controlling stability of nano particles leads to form a microstructure with controlled grain size and porous distribution, which enhances porous burner efficiency.

1. Introduction

The transition from fossil to green economy (low-carbon energy system) depends on innovative processes to generate, share and save energy. According to the International Energy Agency (IEA) to provide universal access to energy by modern energy technologies is one of the greatest challenges of this century [1,2].

Based on the context of green economy [3–8] porous ceramic burners have been shown as a sustainable technology to produce heat and lighting even though by burning low calorific fuels from modern biomass, such as ethanol and biogas [9,10]. Basically the combustion process in a porous ceramic burner consists in heat circulation. The heat comes from the gas to the ceramic solid and it comes from the ceramic solid to the gas [11]. Good review works on porous burners are available in elsewhere [12–16].

With intrinsic proprieties as high thermal stability, high hardness, low density and chemical inertness, ceramic materials such as alumina (Al_2O_3) [17], silicon carbide (SiC) [18], yttria stabilized zirconia (YSZ) [19] have been shown as interesting materials for gas burner applications. Yttrium disilicate ($Y_2Si_2O_7$) exhibits melting point of 1775 °C, stability in oxidant environment and significant optical and mechanical properties [20–22]. Despite of having many advantages, $Y_2Si_2O_7$ has five polymorphs (y, $\alpha \xrightarrow{1225^{\circ}C} \beta \xrightarrow{1445C} \gamma \xrightarrow{1535^{\circ}C} \delta$) [23–26] and the stabilization of each phase has not been consolidated yet. Hence, most of contributions have been aimed on synthesis of $Y_2Si_2O_7$ powders by sol-gel [27], hydrothermal [28] and solid-state reaction [29]. Therefore, many issues on processing of $Y_2Si_2O_7$ have to be investigated.

Colloidal processing is a method to form reliable ceramic components whereby the structure of ceramic suspension is controlled

* Corresponding author.
E-mail addresses: silas.cardoso@usp.br, silascs@ipen.br (S.C. Santos).

http://dx.doi.org/10.1016/j.matchemphys.2016.04.061
0254-0584/

for a desired shape forming. This method is accomplished by a high temperature heat treatment for consolidation of the particles to be satisfied [30–32]. In recent work, Santos et al. [33], developed β-$Y_2Si_2O_7$ reticulated ceramics from biotemplating of the vegetable sponge gourd of Luffa Cylindrica. The sponge architecture is interesting for gas burner design because its reticulated structure can improve gas burning and light emission.

Rare earth doped yttrium disilicate ($Y_2Si_2O_7$:RE) exhibits promising luminescent response. Diaz et al. [34] prepared β-$Y_2Si_2O_7$:Dy^{3+} nanoparticles, which light emission was 40% of the Y_2O_3:Eu^{3+}. GONZALÉZ et al. [35] observed white, red and green light emission from $Y_2Si_2O_7$:Ce^{3+},Tb^{3+}; $Y_2Si_2O_7$:Eu^{3+} and $Y_2Si_2O_7$:Tb^{3+} respectively. Considering the experience from our previous work on colloidal processing of β-$Y_2Si_2O_7$ [33] and bio-prototyping [36], the present study aims to obtain dysprosium doped yttrium disilicate porous burner prototype from bio-templating of Luffa Cylindrica. The effects of particle size-shape, viscosity of suspension, bio-template architecture and thermal treatment on the formation a porous microstructure of the burner prototype are reported. In addition, thermoluminescent response and radiation efficiency of the burner prototype are evaluated.

2. Experimental

By hydrothermal method [33] β-$Y_{1.95}Dy_{0.05}Si_2O_7$ powders with pycnometric density (ρ) of 4.04 g cm^{-3} and specific surface area (SSA) of 10.9 m^2 g^{-1} were produced.

The mean particle size (d_{50}) was measured by means of Photon Correlation Spectroscopy (PCS, ZetaPALS Analyzer, Brookhaven Instruments). For PCS measurements an aqueous suspension with 0.01 vol% solids at pH 10, which is a good condition to disperse particles [33], was prepared. For dispersion of particles tetraethylammonium hydroxide (TMAH, Sigma-Aldrich) was used as deflocculant. The homogenization of ceramic suspensions was performed on a ball mill for 24 h.

Zeta potential (ζ) in aqueous medium was evaluated with a light scattering analyzer (ZetaPALS, Brookhaven Instruments Corporation). Stock suspensions with 0.5 g L^{-1} solids were prepared with NaCl 10^{-3} M as an indifferent electrolyte. HCl and KOH solutions were used to set the pH of the stock suspensions from acid to alkaline condition (pH 5.6–12). Further, 0–3 wt% of polyacrylic ammonium acid (PAA, Duramax D3005) was added to the stock solution. All suspensions were homogenized in an ultrasound cleaner for 2 min (Dr.Hielscher 400US).

The stabilization parameters for yttrium disilicate suspensions are from our previous work [33]. Therefore, β-$Y_{1.95}Dy_{0.05}Si_2O_7$ suspensions with 25 vol% were prepared with tetramethylammonium hydroxide (TMAH, Sigma-Aldrich), 1 wt% PAA, 0.4 wt% CMC (carboxymethyl-cellulose, Sigma-Aldrich). All suspensions were homogenized in a ball mill for 24 h, using alumina spheres ($Ø_{spheres}$ = 10 mm).

The flow behavior of β-$Y_{1.95}Dy_{0.05}Si_2O_7$ suspensions was evaluated with a rheometer (Haake RS600, Thermo Scientific). The sensor system consisted of a double-cone rotor and a stationary plate (DC60/1°). The flow behavior of the suspensions was characterized in the control rate mode (CR) and compared with rheological models available in rheometer database (Haake Rheowin Data Manager v. 3.61.0.1). All measurements were evaluated at 25 °C by increasing the shear rate ($\dot{\gamma}$) from 0 to 1000 s^{-1} in 5 min, holding for 2 min at 1000 s^{-1} and returning to 0 s^{-1} in 5 min. For each CR step 200 points were measured.

The sponge gourd (Luffa Cylindrica, LCy) was used as a template. LCy was cut and shaped like a bulb lamp (40 × 40 × 10 mm). Immersion of samples was performed in β-$Y_{1.95}Dy_{0.05}Si_2O_7$ suspension for 30 min (optimized time) [37]. After the excess ceramic material had been squeezed out, the samples were dried at environmental temperature for 24 h. The impregnated samples were sintered in a vertical furnace (Lindberg/Blue M), where the thermal treatment conditions were based on thermal and gravimetric analysis (TGA/TDA) results of LCy fibers. The microstructure of the sintered samples was evaluated with scanning electron microscopy (MEV, TM3000 Hitachi and MEV, INCAx-act Oxford Instruments).

The performance of the ceramic burner prototype was evaluated by means of the radiant efficiency (N_{rad}), which consists in the ration between the chemical energy from the fuel and thermal energy from the porous structure (Equation (1)) [38]. For gas burning test methane (CH_4, 99.5%, 150 kgf cm^{-2}, ΔH_L = 6.200 Kcal kg^{-1}, White Martins, Brazil) and butane (C_2H_{10}, 99.5%, 2.2 kgf cm^{-2}, ΔH_L = 11.900 Kcal kg^{-1}, White Martins, Brazil) gases were used as fuels. To measure the burner temperature during operation an optical pyrometer (Minipa, MP 350, T_{max} = 700 °C, Δ_T = ±2 °C) was used. The basic set-up performed to measure Nrad is illustrated in Fig. 1.

$$\mathbf{Nrad} = \left(\frac{Qrad}{v_g.\Delta H_L}\right) \times 100\ [\%] \quad (1)$$

where,

- Qrad = τ. T^4 [W m^{-2}];
- τ = 5.6697.10^{-8} W m^{-2} K^{-4} (Boltzmann constant);
- T = Temperature [K];
- V_g = fuel flow [cm^3 min^{-1}];
- ΔH_L = calorific fuel power [kcal kg^{-1}];

Thermoluminescence (TL) measurement of β-$Y_{1.95}Dy_{0.05}Si_2O_7$ particles was performed on a thermoluminescence reader (Risø TL/OSL-DA-20) based on a heating condition up to 700 °C and a spectrometer (Ocean Optics, model QE65 Pro) with spectral sensibility from 200 to 950 nm. The samples were heated at a heating rate of 2 °C s^{-1} up to 400 °C in nitrogen atmosphere. Before TL measurements, samples were irradiated with γ dose 2 kGy using ^{60}Co.

3. Results and discussion

Fig. 2a shows the mean particle size distribution of $Y_{1.95}Dy_{0.05}Si_2O_7$ particles measured by PCS. As a result, β-$Y_{1.95}Dy_{0.05}Si_2O_7$ particles exhibited a narrow particle distribution with mean diameter (d_{50}) of 242 nm, whereas the theoretical diameter (d_{BET}) was 35.7 nm. This significant size difference was

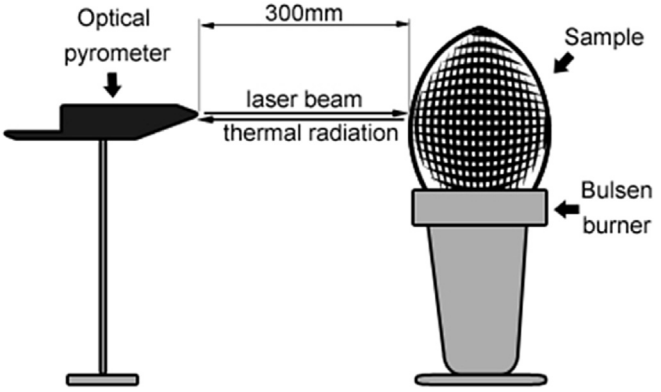

Fig. 1. Basic diagram of set-up performed to evaluate radiant efficiency of β-$Y_{1.95}Dy_{0.05}Si_2O_7$ burner prototype.

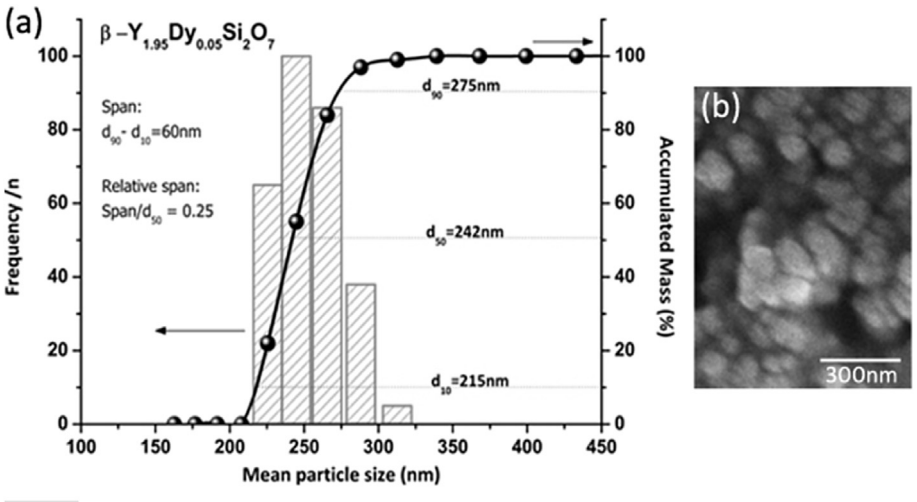

Fig. 2. Characterization of β-$Y_{1.95}Dy_{0.05}Si_2O_7$ nanoparticles (a) mean particle size distribution by means of PCS and (b) particle size and morphology by SEM.

due to the agglomerated state of particles, in which the agglomeration factor (Fag) was 6.8. Besides, the size difference (Span) between minor (d_{10}) and major (d_{90}) distributions was 60 nm, which is a quarter of d_{50}. Furthermore, relating Span to d_{50} (relative span) the difference is much less 0.25. Therefore, β-$Y_{1.95}Dy_{0.05}Si_2O_7$ powders showed narrow particle size distribution, which is desirable for colloidal processing of ceramic suspensions.

Particle characteristics have a significant effect on ceramic processing such as, packing density, size and shape of pore interstices, flow (rheology), and drying, as well as microstructure [39]. In our prior work [33] stable suspensions based on 30 vol% β-$Y_2Si_2O_7$ (d_{50} = 97 nm) with shear thinning behavior were prepared. In Fig. 2b is shown a SEM micrograph of β-$Y_2Si_2O_7$ nanoparticles. As it is seem ceramic nanoparticles are composed of agglomerates of particles whose size was around 50 nm. Particles that present colloidal size distribution are ruled by surface forces and tend to agglomerate easily.

Zeta potential curves of β-$Y_{1.95}Dy_{0.05}Si_2O_7$ as a function of pH and PAA are shown in Fig. 3a. With consideration that the occurrence of hydrolysis and solubility of rare earths is in acid condition [40], the pH range was set from 5.5 to 12. Suspensions with no dispersant (0 wt%PAA) exhibited isoelectric point (IEP) at pH 8.3, an intermediate value as compared to Y_2O_3 and SiO_2 pH_{IEP} = 8–9 and pH_{IEP} = 8–9 respectively [32]. At IEP zeta potential is zero (ζ = 0 mV) and therefore attraction forces are intense, leading particles to agglomerate. Thus, it is desirable to set pH far from IEP in order to prepare stable suspensions. For all pH range the stability condition of β-$Y_2Si_2O_7$ nanoparticles was reached at pH < 7 (|ζ| = 50 mV) and pH ≥ 9.5 (|ζ| = 40 mV).

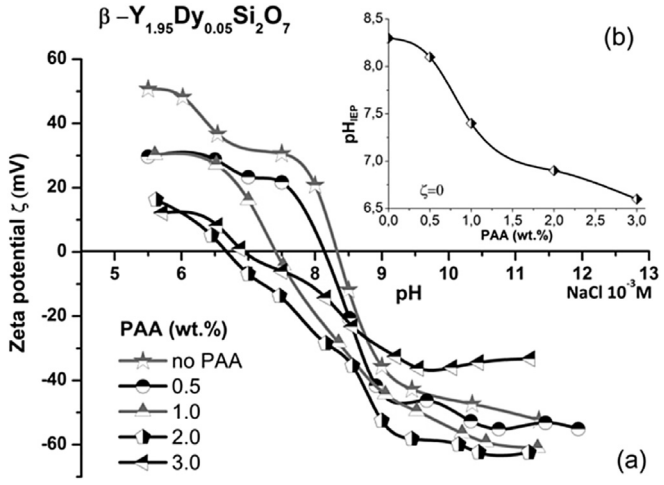

Fig. 3. Stability evaluation of β-$Y_{1.95}Dy_{0.5}Si_2O_7$ in aqueous medium: (a) zeta potential curves as function of pH and PAA, (b) displacement of isoelectric point (IEP) according to PAA dosage.

The addition of PAA was useful to promote larger pH range of stability, displacing IEP from 8.3 to 6.3 (Fig. 3b). The stabilization of particles was improved through absorption of high charged polymer chains on particle surface (electrostatic mechanism) and through physical barrier due to sketched polymer chains (steric mechanism) [32]. Suspensions with 0.5 wt% PAA exhibited an IEP at pH 8.1 and conditions of stability at pH < 7.5 (|ζ| = 30 mV) and pH ≥ 8.5 (|ζ| = 25 mV). Besides, the stability of β-$Y_{1.95}Dy_{0.05}Si_2O_7$ particles was more significant at pH 10, resulting high zeta potential value (|ζ| = 58 mV). For 1 wt% PAA, IEP was displaced from 8.3 to 7.4 and conditions of stability were reached at pH 6–7 and pH ≥ 8.5. For 2 wt% PAA the displacement of IEP was remarkable from 8.3 to 6.9 and a wide range of stability was reached from pH 8. The utmost zeta potential (|ζ| = 60 mV) was observed at pH 10. However, the use of 3 wt% PAA promoted an increase on ionic strength of medium and decreased the repulsion forces between particles consequently. In conclusion, the use of 2 wt% PAA and pH 10 (|ζ| = 60 mV) were the most suitable parameters to prepare high stable suspensions for replica method.

Fig. 4 shows the image by SEM of the LCy template used for production of biomorphic ceramic components. The vegetable sponge of pycnometric density ρ = 1.55 g cm^{-3} exhibits a reticulated structure (Fig. 4a), and fibers in random disposition like a web (Fig. 4b). Fibers presented a mean diameter $ø_f$ = 60 μm and a specific surface area SSA = 22.5 m^2 g^{-1}. Considering that vegetable fibers are composed of fibrils, which are joined together by a vegetal resin tissue the alkaline treatment with 2 wt% NaOH at 60 °C for 2 h was useful to remove surface substances e.g. cellulose, and as a result microchannels and scratches were visible on fibers surface (Fig. 4c). Similar results were observed for TANOBE et al. [41] study as using 2 wt% NaOH at 100 °C for 1.5 h. The difference between these parameters may be associated with the type of vegetable sponge, type of soil, climate conditions and age of plant. The chemical treatment used in this work was suitable to clean the fibers surface and to adequate the LCy template for impregnation.

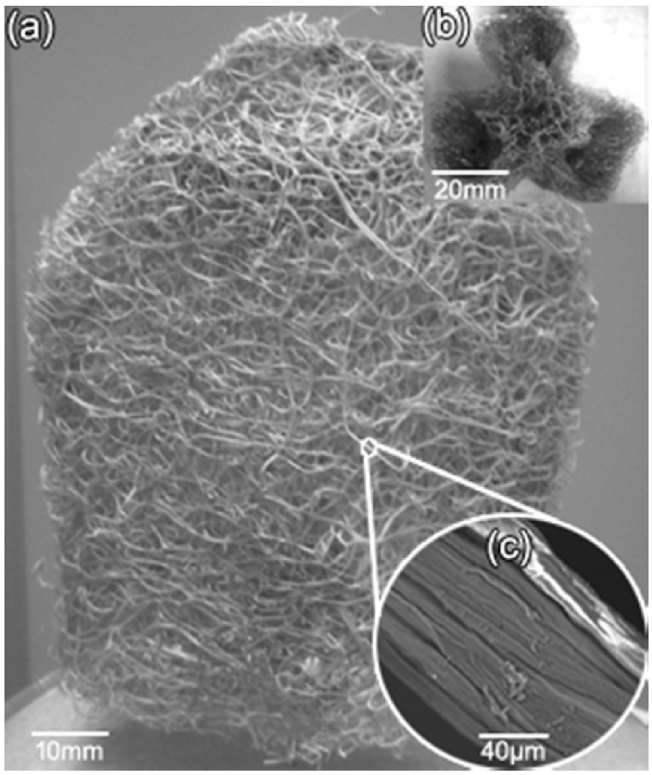

Fig. 4. Sponge gourd Luffa Cylindrica (LCy) used as replica template; (a) macroscopic view of sponge showing its fibrous core and hollows; micrographs of the vegetable fibers by SEM (b) reticulated architecture; (c) fibers surface after alkali treatment with 2 wt% NaOH, revealing surface microchannels.

Based on our previous work [33], yttrium disilicate suspensions with 25 vol% solids content, pH 10, 1 wt% PAA, and 0.4 wt%CMC exhibited suitable viscosity for replica method. From this parameters $Y_{1.95}Dy_{0.05}Si_2O_7$ suspension was prepared and its rheological behavior in CR mode is shown in Fig. 5a. According to results the viscosity (η) decreased as a function of shear rate ($\dot{\gamma}$), which is characteristic of shear thinning suspensions, corresponding to Casson Linear model [32] with the following parameters, apparent

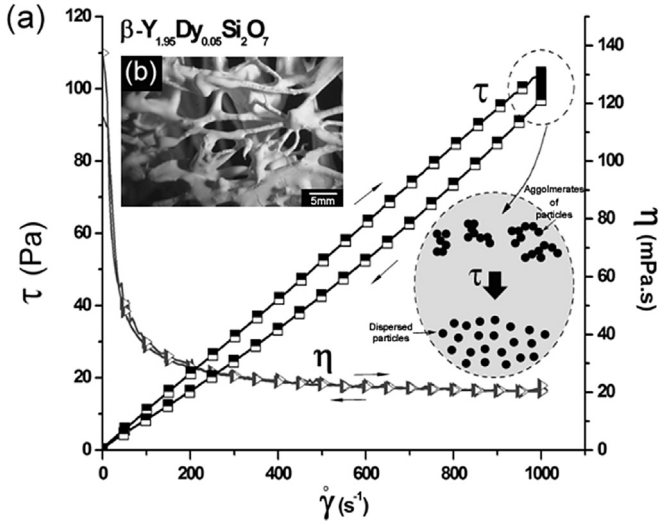

Fig. 5. (a) Flow curves of β-$Y_{1.95}Dy_{0.05}Si_2O_7$ suspensions in CR mode until shear rate of 1000 s^{-1} and (b) optical image of LCy template impregnated using this suspension.

viscosity (η) 473 mPa s, initial tension (τ_0) 0.5673 Pa and plastic viscosity (η_p) 12.37 mPa s. For shear thinning suspensions the proportionality between shear stress (τ) and shear rate ($\dot{\gamma}$) is not satisfied anymore. Shear thinning suspensions present low viscosity when an external force is applied and high viscosity when it is in static condition. Shear thinning behavior is important for many applications such as, painting, bombing, spraying, impregnation and casting [32].

At 1000 s^{-1} $Y_{1.95}Dy_{0.05}Si_2O_7$ suspension exhibited minimum viscosity of 370 mPa s (Fig. 5b). Upon impregnation tests suspensions prepared with 0.4% CMC led to smoothed impregnation of the LCy surface template and preserved its original morphology and reticulated structure. In addition, impregnated samples presented the whole surface impregnated with a thick ceramic layer and closed cavities. Therefore, the use of 0.4 wt% CMC leads the formation of shear thinning suspensions with suitable viscosity for impregnation method.

The $Y_{1.95}Dy_{0.05}Si_2O_7$ gas burner prototype sintered at 1500 °C for 7 h is shown in Fig. 6. The final component (Fig. 6a) exhibited loss weight around 6% compared to green body, pycnometric density $\rho = 3.23$ g cm^{-3} (80% of theoretical density), reticulated morphology and no apparent cracks. Surface fiber is composed of spherical porous smaller than 1 μm as shown in Fig. 6b. The porous microstructure is due to the burning out of the LCy template, as well as the impregnation of a flocculated suspension. As CMC binder dissolves in water, its macromolecules can be adsorbed on two or more particles, leading to flocculation of particles by bridge mechanism. As sintered the agglomerates form porous microstructure. In addition, it is observed that the silicate fiber is composed of ceramic wafers (Fig. 6c), which exhibit internal porous microstructure (Fig. 6d) and heterogeneous distribution of grains.

For gas burner technology, reticulated-porous structures enable higher burning efficiency than solid components, seeing that porous structures act as a heat circulator. Heat recirculation in a porous ceramic is based on heat transfer—conduction (1,2), convection (3) and radiation (4), as shown Fig. 6e. First, the gas is hotter than the ceramic, and as a result heat is transferred convectively from the hot combustion products to the porous ceramic. Second, the hot ceramic conducts and radiates heat in the upstream direction. Third, the temperature of the ceramic is higher than the gas, leading to a solid-to-gas convective heat transfer. Finally, the incoming gases (air + fuel) are preheated, reaching the ignition temperature necessary to continue the heat circulation cycle.

Radiant efficiency (N_{rad}) is the capacity of a porous structure to convert chemical energy from the fuel into heat (thermal energy). Fig. 7 shows N_{rad} results for the β-$Y_{1.95}Dy_{0.05}Si_2O_7$ prototype as a function of the temperature of ceramic burner and the gas used. For CH_4 and C_4H_{10} gases, the N_{rad} increased according to temperature and was maximum at 700 °C. Based on these conditions, CH_4 gas supplied a promising efficiency $N_{rad} = 13\%$, whereas for C_4H_{10} gas $N_{rad} = 12\%$. On the other hand, the use of C_4H_{10} gas was useful to improve the burner temperature (675 °C). In addition a tendency of N_{rad} increment was observed. Qiu et al. [38] using Yb_2O_3:CeO_2 porous burner achieved $N_{rad} = 13\%$.

Fig. 8a shows the TL spectra of β-$Y_2Si_2O_7$ as a function of temperature and wavelength. For β-$Y_2Si_2O_7$ particles no emission of visible light was observed ($\lambda = 350–750$ nm). The emission peak was observed in infrared range ($\lambda = 750–4300$ nm) at 1000 nm and at 400 °C. In addition, its behavior is similar to a blackbody [42]. Apart from 200 °C a solid begins to emit radiation in a continuous spectra, whose intensity increases as a function of temperature increase. As a result, part of the radiation emitted is not visible for human eyes (ultraviolet and infrared range) and only a fraction of it can be observed as visible light [43].

For β-$Y_{1.95}Dy_{0.05}Si_2O_7$ particles (Fig. 8b) the TL emission was

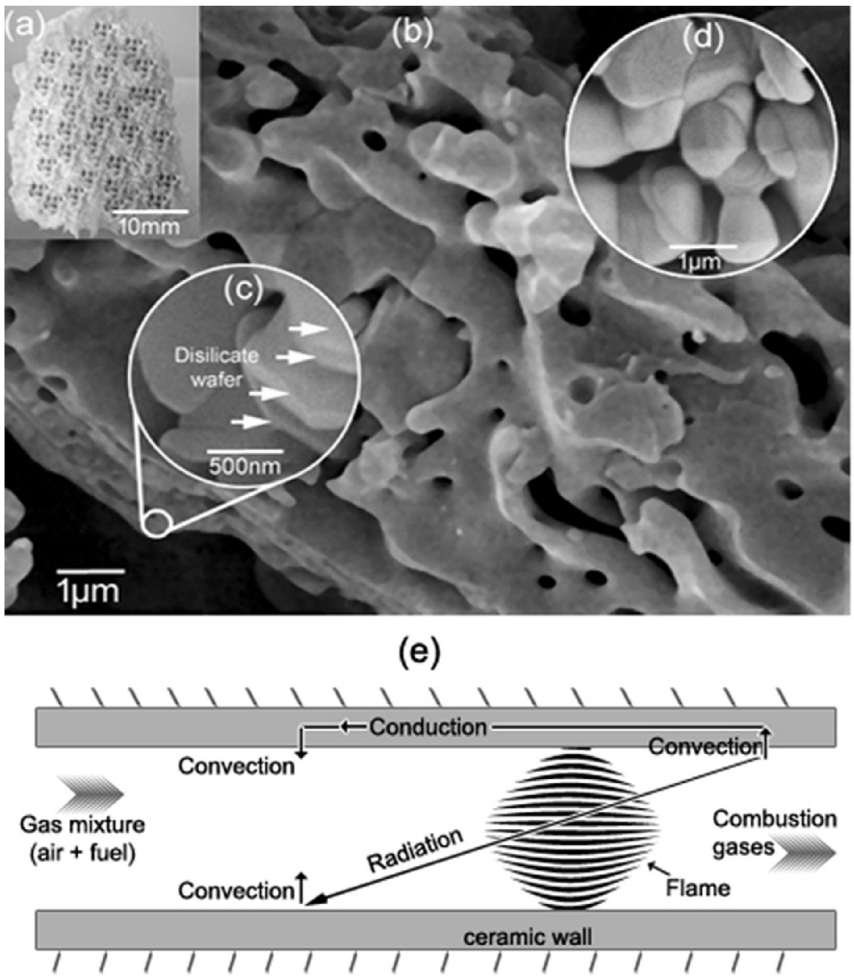

Fig. 6. Biomorphic ceramic of $Y_{1.95}Dy_{0.05}Si_2O_7$ sintered at 1500 °C for 7 h in air; (a) optical image of the gas burner prototype; SEM images of (b) porous fiber surface microstructure; (c) magnification of the wafers on fiber surface (d) internal microstructure of the ceramic fiber composed with heterogeneous grain-size; (e) schematic representation of heat recirculation in a porous ceramic.

remarkable. At 180 °C a TL peak with wavelength of 580 nm, which corresponds to yellow color was observed. Therefore TL response of yttrium disilicate is associated with Dy^{3+} activator ion. Yttrium and dysprosium are trivalent RE (Y^{3+} and Dy^{3+}) and exhibit similar ionic radius, and therefore Dy^{3+} ions replace Y^{3+} ones in crystal structure as substitutional doping. In addition doping Dy^{3+} ions led to higher concentrations of crystal defects as anion vacancies which might resulted in F center luminescence. From TL theory, ionizing radiation creates electron–hole pairs in crystal structure. The electrons can be trapped at dosimetric traps or recombine with F centers at recombination centers. By thermal stimulation the electrons are freed from the dosimetric traps and recombine with the F centers resulting in the 580 nm emission.

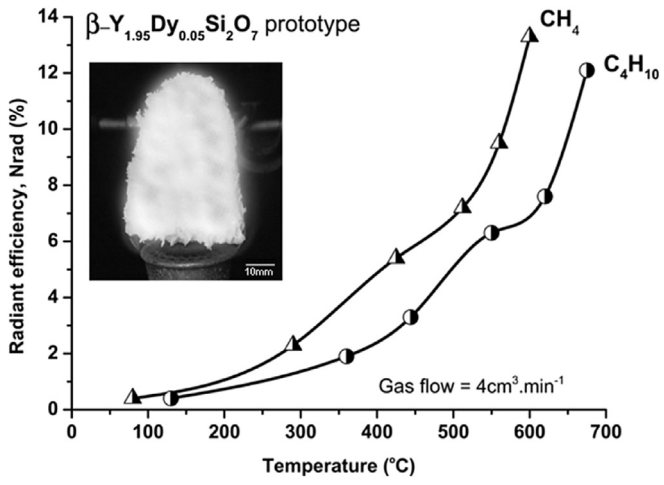

Fig. 7. Radiant efficiency of the β-$Y_{1.95}Dy_{0.05}Si_2O_7$ porous burner prototype as a function of temperature and gas.

According to the Commission International de l'Eclairage (CIE) the yellow color is suitable for lighting in internal environment, in which conditions of comfort and welfare are desired [44]. For β-$Y_{1.95}Dy_{0.05}Si_2O_7$ the TL response exhibited at 180 °C is new in literature. QIU et al. [38] using a gas burner prototype based on Yb_2O_3:CeO_2 observed white light at 500 °C. GONZALÉZ-ORTEGA et al. [35] through ultraviolet stimulation observed three color intense emissions, white, red and green for $Y_2Si_2O_7$:Ce^{3+}:Tb^{3+}, $Y_2Si_2O_7$:Eu^{3+} and $Y_2Si_2O_7$:Tb^{3+} respectively.

4. Conclusion

In the present work a biomorphic ceramic burner prototype with radiant efficiency of 13% and thermoluminescent response at 180 °C and λ = 580 nm was developed by colloidal processing of

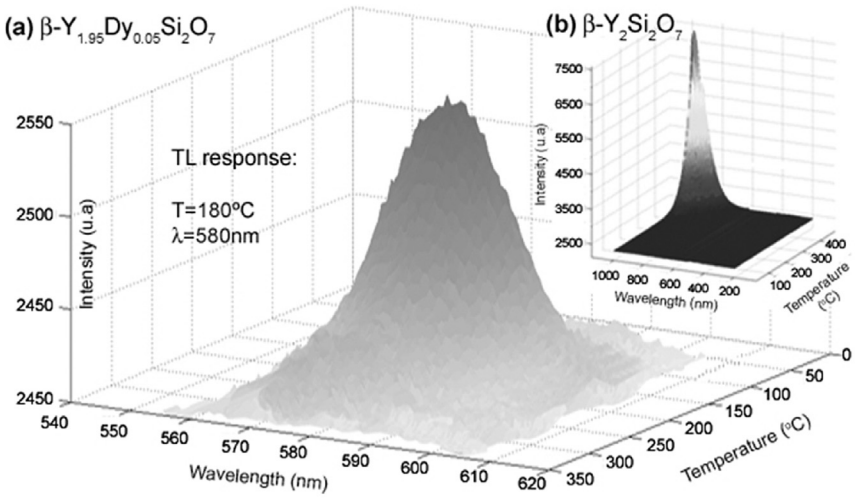

Fig. 8. Thermoluminescence response of (a) β-$Y_{1.95}Dy_{0.05}Si_2O_7$ and (b) β-$Y_2Si_2O_7$ nanoparticles for a heating rate of 2 °C s^{-1} until 400 °C in nitrogen atmosphere. The TL behavior of β-$Y_2Si_2O_7$ was analogue to black body radiation, whereas for β-$Y_{1.95}Dy_{0.05}Si_2O_7$ the TL response was observed at 180 °C and $\lambda = 580$ nm.

beta dysprosium doped yttrium disilicate (β-$Y_{1.95}Dy_{0.05}Si_2O_7$) and from biotemplating of the vegetable sponge Luffa Cylindrica. Shear thinning suspensions with suitable apparent viscosity for replica method were prepared with 25 vol% solids, pH 10, 2 wt% dispersant and 0,4 wt% binder. Alkali treatment of the vegetable fibers with 2 wt%NaOH at 60 °C for 2 h was useful to prepare the biotemplating surface for replica method. Using high temperature treatment at 1500 °C for 7 h in air, β-$Y_{1.95}Dy_{0.05}Si_2O_7$ biomorphic burner prototype with reticulated architecture, porous microstructure and pycnometric density of 3.23 g cm^{-3} (80% theoretical density) was produced.

Acknowledgements

We authors are deeply grateful to Dr. Wilson Acchar, Dr. Francisco Braga, Dr. Thomaz Augusto Restivo, Dr. Linda Caldas, Dr. Maira Tiemi Yoshizumi, MSc. Douglas Will Leite, and MSc. William Naville. In addition, grant #2014/23621-3, São Paulo Research Foundation; National Council for Scientific and Technological Development; and Coordination for Improvement of High Degree People (CAPES).

References

[1] I.E.A. International Energy Agency, Key World Statistics, Key World Statistics, International Energy Agency, I. E. A, Paris, 2013.
[2] I.E.A. International Energy Agency, Energy Technology Perspectives 2015, International Energy Agency, I.E.A, Paris, 2015, p. 418.
[3] T. Wanner, The new 'passive revolution' of the green economy and growth discourse: maintaining the 'sustainable development' of neoliberal capitalism, New Polit. Econ. 20 (2015) 21–41.
[4] D. Gibbs, K. O'Neill, The green economy, sustainability transitions and transition regions : a case study of Boston, Geogr. Ann. B 96 (2014) 201–216.
[5] J.M. Borel-Saladin, I.N. Turok, The green economy: incremental change or transformation? Environ. Policy Gov. 23 (2013) 209–220.
[6] S. Gurtowski, Green economy idea - limits, perspectives, implications, Probl. Ekorozw. 6 (2011) 75–82.
[7] E. Barbier, The policy challenges for green economy and sustainable economic development, Nat. Resour. Forum 35 (2011) 233–245.
[8] A. Hamdouch, M.H. Depret, Policy integration strategy and the development of the 'green economy': foundations and implementation patterns, J. Environ. Plann Man. 53 (2010) 473–490.
[9] A. Hublin, D.R. Schneider, J. Dzodan, Utilization of biogas produced by anaerobic digestion of agro-industrial waste: energy, economic and environmental effects, Waste Manage Res. 32 (2014) 626–633.
[10] I.E.A. International Energy Agency, Tracking Clean Energy Progress 2015, Tracking Clean Energy Progress, International Energy Agency, I.E.A, Paris, 2015, p. 98.
[11] A.J. Barra, J.L. Ellzey, Heat recirculation and heat transfer in porous burners, Combust. Flame 137 (2004) 230–241.
[12] K. Vafai, Handbook of Porous Media, 2 ed., Taylor & Francis, 2005.
[13] S.K. Chou, W.M. Yang, J. Li, Z.W. Li, Porous media combustion for micro thermophotovoltaic system applications, Appl. Energy 87 (2010) 2862–2867.
[14] M.A. Mujeebu, M.Z. Abdullah, M.Z.A. Bakar, A.A. Mohamad, R.M.N. Muhad, M.K. Abdullah, Combustion in porous media and its applications – a comprehensive survey, J. Environ. Manag. 90 (2009) 2287–2312.
[15] M.A. Mujeebu, M.Z. Abdullah, M.Z.A. Bakar, A.A. Mohamad, M.K. Abdullah, Applications of porous media combustion technology – a review, Appl. Energy 86 (2009) 1365–1375.
[16] S. Wood, A.T. Harris, Porous burners for lean-burn applications, Prog. Energ Combust. 34 (2008) 667–684.
[17] A.M. Herrera, O. Alvarez, J. Escobar, V. Moreno, A.A.M. Oliveira, D. Hotza, Fabrication and characterization of alumina foams for application in radiant porous burners, Materia Rio De. Jan. 17 (2012) 973–987.
[18] K.T. Mueller, O. Waters, V. Bubnovich, N. Orlovskaya, R.H. Chen, Super-adiabatic combustion in Al2O3 and SiC coated porous media for thermoelectric power conversion, Energy 56 (2013) 108–116.
[19] S.Y. Gomez, J.A. Escobar, O.A. Alvarez, C.R. Rambo, A.P.N. de Oliveira, D. Hotza, ZrO2 foams for porous radiant burners, J. Mater Sci. 44 (2009) 3466–3471.
[20] J.M. Kim, H.J. Lee, K.P. Kim, J.S. Yoo, Optical characteristics of polymorphic Y(2-x)Si(2)O(7):Eu(x)(3+) crystal for lamp application, J. Electrochem Soc. 155 (2008) E189–E192.
[21] Z. Sun, Y.C. Zhou, J.Y. Wang, M.S. Li, gamma-Y2Si2O7, a machinable silicate ceramic: mechanical properties and machinability, J. Am. Ceram. Soc. 90 (2007) 2535–2541.
[22] I.A. Bondar, Rare-earth silicates, Ceram. Int. 8 (1982) 83–89.
[23] K.T. Liddell, D.P. Thompson, X-ray diffraction data for yttrium silicates, Br. Ceram. Trans. J. 85 (1986) 17–22.
[24] J. Felsche, Polymorphism and crystal data of the rare-earth disilicates of type R.E.2Si2O7, J. Less Common Metals 21 (1970) 1–14.
[25] J. Felsche, W. Hirsiger, The polymorphs of the rare-earth pyrosilicates R.E.2Si2O7, [R.E.: La, Ce, Pr, Nd, Sm], J. Less Common Metals 18 (1969) 131–137.
[26] I.A. Bondar, Phase transformations in complex oxides of rare earth elements, Thermochim. Acta 92 (1985) 517–520.
[27] M. Diaz, I. Garcia-Cano, S. Mello-Castanho, J.S. Moya, M.A. Rodriguez, Synthesis of nanocrystalline yttrium disilicate powder by a sol-gel method, J. Non Crystalline Solids 289 (2001) 151–154.
[28] P.A. Trusty, K.C. Chan, C.B. Ponton, Synthesis of sinteractive single-phase microstructure yttrium disilicate precursor powder using hydrothermal processing, J. Mater Res. 13 (1998) 3135–3143.
[29] Z.Q. Sun, Y.C. Zhou, M.S. Li, Low-temperature synthesis and sintering of gamma-Y2Si2O7, J. Mater Res. 21 (2006) 1443–1450.
[30] Colloidal processing of ceramics, J. Am. Ceram. Soc. 83 (2000) 2341–2359.
[31] F.F. Lange, Colloidal processing of powder for reliable ceramics, Curr. Opin. Solid St. M. 3 (1998) 496–500.
[32] R. Moreno, Reología de suspensiones cerámicas, Consejo Superior de Investigaciones Científicas, Madrid, 2005.
[33] S.C. Santos, C. Yamagata, A.C. Silva, L.F.G. Setz, S.R.H. Mello-Castanho, Yttrium disilicate micro-cellular architecture from biotemplating of luffa cylindrica, J. Ceram. Sci. Technol. 5 (2014) 203–208.
[34] M. Diaz, C. Pecharroman, F. del Monte, J. Sanz, J.E. Iglesias, J.S. Moya, C. Yamagata, S. Mello-Castanho, Synthesis, thermal evolution, and luminescence properties of yttrium disilicate host matrix, Chem. Mater 17 (2005)

1774–1782.
[35] J.A. Gonzalez-Ortega, N. Perea, G.A. Hirata, White light emission from Y2SiO5 : Ce, Tb films excited by electroluminescence, Opt. Mater 29 (2006) 47–50.
[36] S.C. Santos, C. Yamagata, L.L. Campos, S.R.H. Mello-Castanho, Bio-prototyping and thermoluminescence response of cellular rare earth ceramics, J. Eur. Ceram. Soc. 36 (2016) 791–796.
[37] S.C. Santos, C. Yamagata, W. Acchar, S.R.H.M. Castanho, Yttria nettings by replica processing, Mater. Sci. Forum 798 (2014) 3.
[38] K. Qiu, A.C.S. Hayden, Premixed gas combustion stabilized in fiber felt and its application to a novel radiant burner, Fuel 85 (2006) 1094–1100.
[39] J. Reed, Principles of Ceramics Processing, 2 ed., John Wiley & Sons, New York, 1995.
[40] J.J. Ryszard Sprycha, Egon Matijevic, Zeta potential and surface charge of monodispersed colloidal yttrium (III) oxide and basic carbonate, J. Colloid Interface Sci. 149 (1991) 562–568.
[41] V.O.A. Tanobe, T.H.D. Sydenstricker, M. Munaro, S.C. Amico, A comprehensive characterization of chemically treated Brazilian sponge-gourds (Luffa cylindrica) (vol 24, pg 474, 2005), Polym. Test. 29 (2010) 288–289.
[42] D.R. Vij, Luminescence of Solids, Plenum Press, New York, 1998.
[43] A.J.J. Bos, Theory of thermoluminescence, Radiat. Meas. 41 (Supplement 1) (2006) S45–S56.
[44] C.I.E. International Commission on illumination, Lighting of Work Places Part 1: Indoor, International Commission on illumination, Austria, 2001.